

Seasonal Prediction of Tropical Cyclone Frequency over the East China Sea through a Bayesian Poisson-Regression Method

Chang-Hoi Ho¹, Hyeong-Seog Kim¹, and Pao-Shin Chu²

¹*School of Earth and Environmental Sciences, Seoul National University, Seoul, Korea*

²*Department of Meteorology, University of Hawaii, Hawaii, USA*

(Manuscript received 11 September 2008; in final form 31 December 2008)

Abstract

In this study, a Bayesian method has been used to predict the seasonal number of tropical cyclones (TCs) over the East China Sea (25°N–35°N, 120°E–130°E). The method considers two periods each year and provides several different predictions of the number of TCs that will enter the target area during a typhoon season, assigning a probability value to indicate the likelihood of each prediction. The method was used to forecast the number of TCs that would occur over the extended season (June–September) issued by June 1 and over the peak season (July–September) issued by July 1. The three parameters of sea surface temperature (SST), outgoing longwave radiation (OLR), and 850-hPa vorticity (VOR850) were used as predictors, based on lag correlation coefficients with the TCs over the target region for 1979–2003. For the extended season prediction, the SST for February–April, the VOR850 for February 16–May 15, and the OLR for May 1–May 15 were chosen as predictors in the TC forecast system. The three predictors for the peak season prediction are delayed one month relative to those for the extended season prediction. The observed TCs over the target region mainly fall into the prediction range within 25% probability from the median during the period from 1979 to 2007. The method predicts the mean TC frequency with a high level of accuracy, yielding a correlation coefficient of 0.69 and 0.71 and a root mean square error of 1.48 and 1.20 between the predicted and observed TCs for the extended and peak season forecasts, respectively. This TC prediction method may soon be used for operational purposes.

Key words: Tropical cyclone, seasonal prediction, Bayesian regression, East China Sea

1. Introduction

The landfall of tropical cyclones (TCs) is known to be one of the most serious natural disasters that occur in East Asia. Over the past 10 years (1998–2007), 33 TCs have affected the Korean Peninsula, causing hundreds of deaths and financial losses of \$10 billion (NEMA, 2008). Similar damage resulting from TCs has also been observed in neighboring countries, e.g., China and Japan (Wang *et al.*, 2007; Kim *et al.*, 2005a; Nakazawa, 2006). Normally TC landfalls are associated with damage and fewer TCs would be a blessing. However, TCs are sometimes desirable; the landfall of TCs may provide sufficient water re-

sources to end a long drought, cooling the surface temperature of regions affected by unbearable heat waves, etc.

From the above discussion, it is apparent that reliable long-range forecasting of TC landfall would be advantageous. There are many approaches that use statistical methods to predict basin-wide or regional seasonal TC activity in the western North Pacific. Chan *et al.* (1998, 2001) developed a seasonal forecast method for the western North Pacific region based on the projection pursuit regression technique by using several climatic phenomena such as El Niño and La Niña, cold surge, and polar vortex. Lee *et al.* (2007) constructed a similar forecast method using smart predictors that are combination of potential predictors to achieve the best prediction performance during the hindcast period. Further, Kwon *et al.* (2007) have taken Lee *et al.* (2007)'s method and added the feature of an associated uncertainty measurement that is provided with a single forecast.

Corresponding Author: Chang-Hoi Ho, Climate Physics Laboratory, School of Earth and Environmental Sciences, Seoul National University, Seoul 151-747, Korea.
Phone : +82-2-880-8861, Fax : +82-2-876-6795
E-mail: hoch@cpl.snu.ac.kr

Forecasting TCs becomes very complex when the area considered is decreased from the entire basin to the area of a single nation or a specific seaboard region. This is because TC activities are influenced not only by the genesis locations but also by the preferred tracks, which depend on both local thermodynamics and large-scale dynamics (e.g., Ho *et al.*, 2004; Kim *et al.*, 2005b; Ho *et al.*, 2005). Thus, the accuracy of prediction for a smaller region tends to be lower than that on a basin-wide scale. Despite these inherent difficulties in forecasting TCs, it is necessary to limit the forecast domain to small areas to facilitate efficient disaster preparation (Chan *et al.*, 1998; Liu and Chan, 2003; Chu *et al.*, 2007). With this in mind, Chu *et al.* (2007) developed a method that predicted TC activity for a limited region in the vicinity of Taiwan using multivariate least absolute deviation regression incorporating some environmental predictors, e.g., sea surface temperature (SST), sea level pressure, low-level vorticity, precipitable water, and vertical wind shear. It should be noted that the potential predictors may vary from one region to another.

While most seasonal TC forecasting techniques are based on the deterministic approach, probability forecasts would better express the uncertainty associated with the forecasts. Elsner and Jagger (2006) and Chu and Zhao (2007) independently introduced a Bayesian method for predicting TCs in the Atlantic and central North Pacific, respectively. The methods predict a range of different values for the number of TCs that will occur in a season in the target area and assign probabilities to each predicted TC count, e.g., a 20% probability that exactly 5 TCs will occur, a 50% probability that exactly 6 TCs will occur, and a 30% probability that exactly 7 TCs will occur. This method presents more useful information than previous prediction methods that give only the deterministic TC frequency, e.g., 6 TCs. In addition to making probability statements about forecasts, Bayesian inferences provide an ability to update these statements as new information is received and recognize that the statistical distribution of the TC rate is changing over time rather than forever fixed. The present study uses the Bayesian method to predict TCs during typhoon

season over the East China Sea (ECS) issued on the first day of the season; June 1 for the extended season (June–September) prediction and July 1 for the peak season (July–September) prediction. Since more than half of the TCs that passed the ECS recurved through the Korean Peninsula, the prediction of TC activity in the ECS, the focus of this paper, is of vital interest to Korea and, to some extent, Japan and China.

The structure of this paper is as follows. The data and a brief description of the Bayesian method are given in section 2. The chosen predictand variables and their spatial distributions are described in section 3, and the results of the Bayesian method are discussed in section 4. The conclusions are presented in section 5.

2. Data

The present study used TC data obtained from the Regional Specialized Meteorological Center-Tokyo Typhoon Center. The data contain information on the name, date, position (in latitude and longitude), minimum surface pressure, and maximum wind speed of TCs for every 6-h interval. A TC is categorized as one of three types depending on its 10-min maximum sustained wind speed (w_{max}). These are tropical depression ($w_{max} < 17 \text{ m s}^{-1}$), tropical storm ($17 \text{ m s}^{-1} \leq w_{max} < 34 \text{ m s}^{-1}$), and typhoon ($w_{max} \geq 34 \text{ m s}^{-1}$). In this study, we consider only tropical storms and typhoons. Even though data on TCs since 1951 are available, there are some problems in employing the data in a study; in particular, the positions and intensities of TCs that occurred in the initial years of the study may not be accurate. In addition, the TC tracks in the western North Pacific have experienced decadal changes due to variations in large-scale circulation in the late 1970s (Ho *et al.*, 2004). For these reasons, the data considered in this study is confined to the period 1979–2007.

The climatological distribution of the monthly TC frequency over the ECS (25°N–35°N, 120°E–130°E) shows a single peak in August. There were approximately 0.5 TCs in June, 1 in July, 1.6 in August, 0.8 in September, 0.5 in October, and very few in the other months. Here, June to September is selected as the

period of investigation because the landfalls of TCs or approaches of TCs on the Korean Peninsula seldom occur in October.

SST, outgoing longwave radiation (OLR), and 850-hPa vorticity (VOR850) are chosen as predictors. We use the extended reconstructed SST version 3 (Smith *et al.*, 2007) and daily interpolated OLR data (Liebmann and Smith, 1996) obtained from the website of the National Oceanic and Atmospheric Administration–Climate Diagnostic Center (<http://www.cdc.noaa.gov>). The horizontal resolutions of the SST and OLR are $2^\circ \times 2^\circ$ and $2.5^\circ \times 2.5^\circ$ (in latitude/longitude), respectively. The daily VOR850 values were obtained from the National Centers for Environmental Prediction/Department of Energy Reanalysis-2 (Kanamitsu *et al.*, 2002). Its horizontal resolution is $2.5^\circ \times 2.5^\circ$ (in latitude/longitude). These three climate variables have been used widely, and detailed descriptions are available in many literatures.

3. Predictands, predictors, and prediction method

This section describes the use of TCs as pre-

dictands and that of preceding climate variables as predictors; it also discusses the Bayesian system that we used to make prediction twice a year. That is, the prediction experiment is attempted for the peak typhoon season (July to September) and the forecast is issued by 1st of July. A second experiment is aimed towards the four-month long (June to September) extended season and this forecast is issued by 1st of June. From among many potential predictors, we chose only three climate variables — SST, OLR, and VOR850, considering reliable physical and dynamical connections to TCs over the ECS. These predictors were determined on the basis of lagged correlation analysis between the observed TCs in the target area and large-scale environmental parameters for 1979–2003 and the last 4 years (2004–2007) are reserved as a period independent from the predictor analysis.

a. TCs as predictands

Figure 1 presents the temporal variations in the number of TCs for the extended season (open circle) and for the peak season (open square) across the ECS region. As expected, these two curves are highly cor-

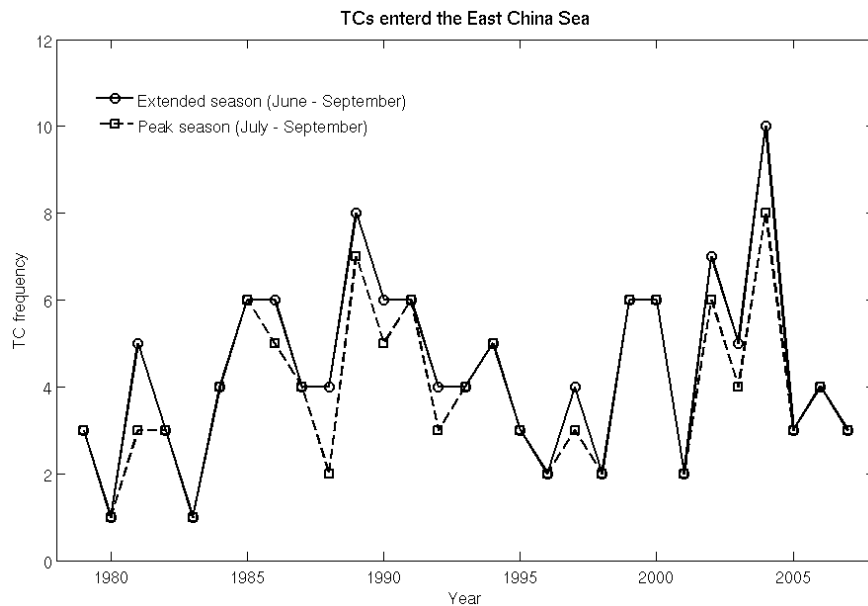


Fig. 1. The time series of frequency of TCs over the East China Sea for the extended season (June–September, open circle) and the peak season (July–September, open square).

related due to the fact that few TCs are observed in June. Their correlation coefficient is 0.95. For the extended season, there is a strong interannual variability with a minimum of one TC in 1980 and 1983 and a maximum of 10 TCs in 2004. Specifically, of the 10 TCs that entered the ECS in 2004, 8 struck Japan (Kim *et al.*, 2005a; Nakazawa, 2006). The average number of TCs for the extended season is 4.4, with a standard deviation of 2.1. Of the 29 years that comprise the study period, 9 have over 5.5 TCs and 10 have fewer than 3.5 TCs. A similar strong interannual variation is also found in the case of the TCs that entered the target area for the peak season. For this period, the average number of TCs is 3.9, with a standard deviation of 1.8.

b. Climate variables as predictors

As stated previously, three climate variables, SST, OLR, and VOR850, were chosen as the input data to be used in the prediction system. These variables should be accessible via the internet prior to the beginning of the prediction experiment. Data are usually provided on the web site two weeks after their collection; this delay precludes the use of very recent data in the operational prediction setting. Accordingly, we used monthly SST data collected up to one month before the earliest date for which it was used to make predictions, and the daily OLR and VOR850 data used was collected up to one-half month before the earliest date for which predictions were made, i.e., SST data up to April and OLR and VOR850 data up to May 15 was used to make the extended season prediction. All data sets may be shifted one month (or less) for the peak season prediction. In the following, two sets of predictors are discussed, one for the extended season forecast made on June 1 and the other for the peak season forecast made on July 1.

Figure 2 shows the lagged-correlation coefficients of the three predictors along with the accumulated TCs for the extended season forecast over the ECS for the period 1979–2003. The light shading denotes regions with highly positive correlation and that the gray shading denotes regions with highly negative correlation, which are all significant at the 95% con-

fidence level. For convenience, these are referred to as critical regions. The remote SSTs averaged for the antecedent February–April over the central to eastern tropical Pacific region are found to have a large, negative lag-correlation with the extended season TC data over the ECS (Fig. 2a). This suggests that

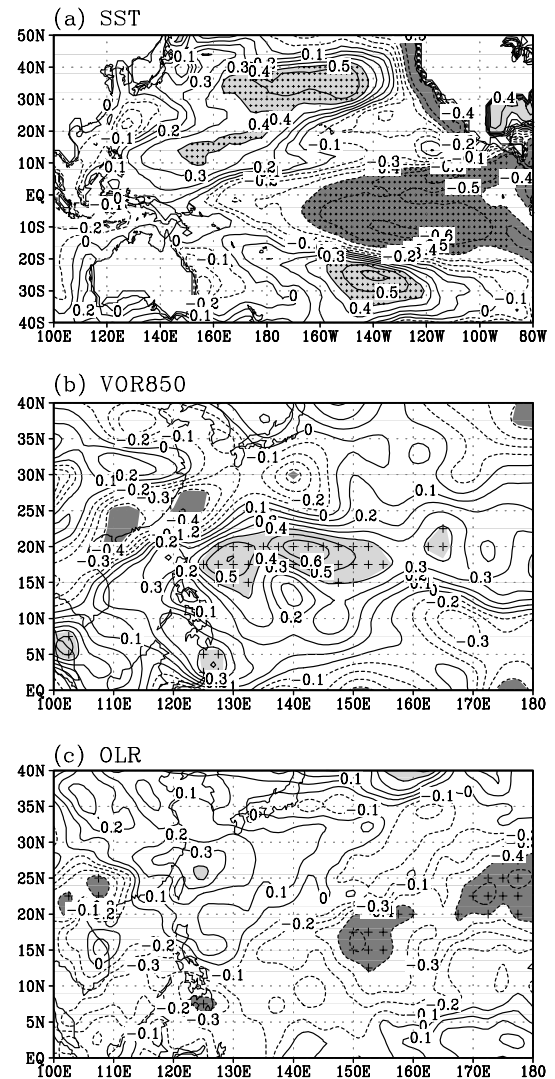


Fig. 2. (a) The spatial distribution of lag-correlation coefficients between the extended season TCs and SST for February–April, (b) same as (a) but for VOR850 for February 16–May 15, and (c) same as (a) but for OLR for May 1–May 15. The light (dark) shading denotes the positively (negatively) correlated region at the 95% confidence level. The cross marks denote the critical regions selected as the potential predictors.

the remote ocean basin, rather than the local western Pacific SST, may play a vital role modulating TC activity over the ECS. This is because changes in the remote SST influence atmospheric circulation over the western North Pacific which then manipulates TC genesis and the steering flows that determine the TC tracks.

Apart from the remote tropical forcings, other critical regions that straddle the central Pacific in both hemispheres with a positive correlation are noted in Fig. 2a. The alternation of positive and negative critical regions in the Pacific forms a wave-like pattern which persists from the preceding mid winter to spring. It is interesting to note that its spatial distribution resembles the variability associated with the El Niño–Southern Oscillation, especially the decaying phase of La Niña (Harrison and Larkin, 1998). An opposite pattern to Fig. 2a is amenable to the decaying phase of El Niño. In general, during La Niña episodes TC genesis locations are shifted northwestward in the WNP (Chu, 2004). Accordingly, TCs tend to pass frequently over the ECS. Based on the lag-correlation pattern between the SSTs in late winter and spring, the aforementioned three regions (with dotted marks) are selected as the predictors. Specifically, the predictor is the sum of the average SST values over the two positively correlated domains minus the average SST value over the negatively correlated domain for the period February–April.

The predictors of VOR850 and OLR are obtained in a similar manner. Figures 2b and 2c show the lagged correlation between the extended season forecasts and the VOR850 and OLR data for February 16 to May 15 and May 1 to May 15, respectively. Regarding the correlation between the TCs and VOR850 (Fig. 2b), a large patch of positive critical regions are found along the subtropics in the western Pacific. Two smaller, negative critical regions are observed over south and eastern China. Broadly speaking, this correlation distribution is observed for the western North Pacific monsoon signal (Wang *et al.*, 2001), indicating a positive vorticity anomaly in the lower troposphere over the core TC genesis region (i.e., the South China Sea and Philippine Sea) in spring that tends to be followed by frequent move-

ments of TCs into the ECS. For the OLR in late spring (Fig. 2c), a negative correlation prevails over the entire western tropical North Pacific. This clearly indicates that the negative OLR anomaly (i.e., active convection) precedes and may persist through the typhoon season, leading to favorable conditions for TC genesis. It is noted that relatively recent information of OLR is used as predictor compared to the VOR850.

Similar to what was done for the extended season (Fig. 2), the lagged-correlation coefficients of the three predictors used for the peak season forecast over the ECS for the same period are depicted in Fig. 3. Because the forecast for peak season is made by July 1, one month later compared to the previous forecast experiment, we will use the predictors for more recent periods: the SST data for March–May and VOR850 and OLR data for March 16–June 15 and June 1–June 15, respectively. Interestingly, the overall distributions of the three predictors for the two periods are quite similar (Figs. 2 and 3). One subtle difference is that the absolute magnitude of the correlation coefficients, particularly over the critical regions, is slightly larger in the shorter (i.e., peak season) season than in the longer (i.e., extended season) season. This slight degradation in the correlation skill implies that relatively few TCs occurred in June are perhaps random in nature and not necessarily related to the peak season activity. Further, expect that the prediction will be more accurate in the peak season when using recent predictors. This will be shown in section 4.

c. Bayesian regression method for TC counts

In this study, we adopt the Bayesian prediction method suggested by Chu and Zhao (2007), which is based on Poisson regression. The distribution of the occurrence of seasonal TCs is generally considered a Poisson process (e.g., Chu and Wang, 1998). The Poisson process is governed by a single parameter, the intensity λ . Given λ (i.e., the mean seasonal numbers of TCs or the so-called TC rate) and h , the number of TCs occurring in a unit of observation time, say one season, the probability mass function (Epstein, 1985) is

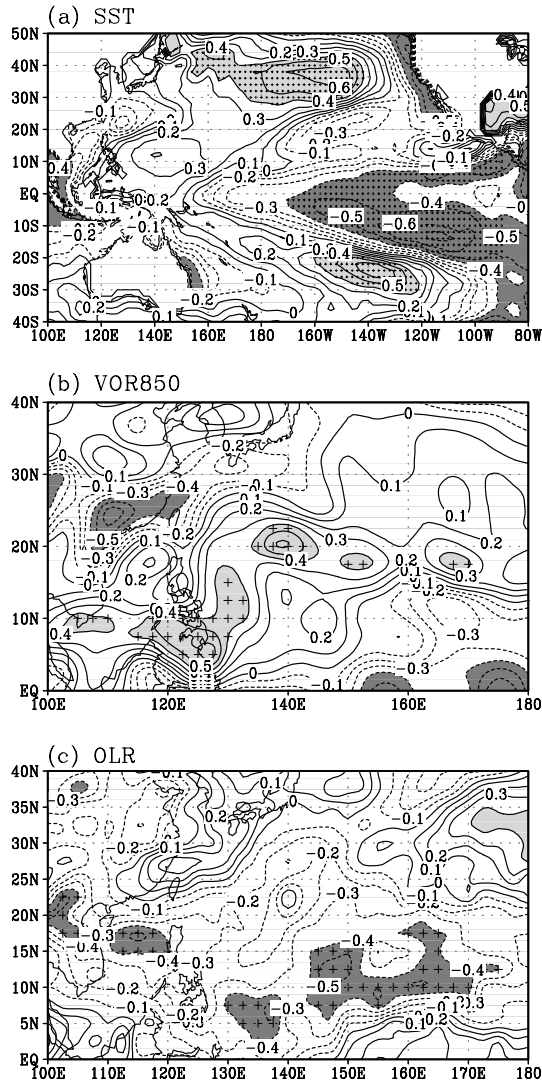


Fig. 3. (a) The spatial distribution of lag correlation coefficient between the peak season TCs and SST for March–May, (b) same as (a) for VOR850 for March–June 15, and (c) same as (a) but for OLR for June 1–June 15.

$$P(h | \lambda) = \exp(-\lambda) \frac{\lambda^h}{h!}, \quad (1)$$

where $h=0,1,2,\dots$ and λ is the Poisson mean, $\lambda > 0$. The Poisson regression model for TC prediction is designed as follows. We assume there are N observations and that for each observation there are K relative predictors. We then define a latent random N -vector \mathbf{Z} such that for each observation h_i , where $i=1,2,\dots,N$, $Z_i = \log \lambda_i$, where λ_i is the relative Poisson intensity for the i -th observation. N denotes the sample size – 29 in this study (1979–2007). The link function between this latent variable and its associated predictors is expressed as $Z_i = \mathbf{X}_i \boldsymbol{\beta} + \varepsilon_i$, where $\boldsymbol{\beta} = [\beta_0, \beta_1, \beta_2, \dots, \beta_K]'$ is a random vector. The noise ε_i is assumed to be identically and independently distributed and also normally distributed with zero mean and σ^2 variance, and $\mathbf{X}_i = [1, X_{i1}, X_{i2}, \dots, X_{iK}]$ denotes the predictor vector. In vector form, the general Poisson linear regression model can be formulated as below:

$$P(\mathbf{h} | \mathbf{Z}) = \prod_{i=1}^N P(h_i | Z_i), \quad (2)$$

where $h_i | Z_i \sim \text{Poisson}(h_i | e^{Z_i})$, $\mathbf{Z} | \boldsymbol{\beta}, \sigma^2, \mathbf{X} \sim \text{Normal}(\mathbf{Z} | \mathbf{X}\boldsymbol{\beta}, \sigma^2 \mathbf{I}_N)$, where, specifically, $\mathbf{X}' = [\mathbf{X}'_1, \mathbf{X}'_2, \dots, \mathbf{X}'_N]$, \mathbf{I}_N is a $N \times N$ identity matrix, $\mathbf{X}_i = [1, X_{i1}, X_{i2}, \dots, X_{iK}]$ is the predictor vector for h_i , $i=1,2,\dots,N$, and $\boldsymbol{\beta} = [\beta_0, \beta_1, \beta_2, \dots, \beta_K]'$. Here, *Normal* and *Poisson* stand for the normal distribution and Poisson distribution, respectively. In Eq. (2), β_0 is referred to as the intercept. Note that the Poisson rate λ is treated as a random variable that is conditional on the predictors.

In Chu and Zhao (2007), the posterior distributions for the hidden variable Z , $\boldsymbol{\beta}$ and σ^2 are explicitly derived using the Bayesian inference as follows:

$$\begin{aligned} Z_i | \mathbf{h}, \boldsymbol{\beta}, \sigma^2 &\sim P(Z_i | \mathbf{h}, \boldsymbol{\beta}, \sigma^2) \propto \exp \left[-e^{Z_i} + Z_i h_i - \frac{1}{2\sigma^2} (Z_i - \mathbf{X}_i \boldsymbol{\beta})^2 \right], \quad i=1,2,\dots,N, \\ \boldsymbol{\beta} | \mathbf{h}, \mathbf{Z}, \sigma^2 &\sim \text{Normal}(\boldsymbol{\beta} | (\mathbf{X}'\mathbf{X})^{-1} \mathbf{X}'\mathbf{Z}, (\mathbf{X}'\mathbf{X})^{-1} \sigma^2), \\ \sigma^2 | \mathbf{h}, \mathbf{Z}, \boldsymbol{\beta} &\sim \text{Scale-Inv-}\chi^2(\sigma^2 | N, \frac{1}{N} (\mathbf{Z} - \mathbf{X}\boldsymbol{\beta})' (\mathbf{Z} - \mathbf{X}\boldsymbol{\beta})). \end{aligned} \quad (3)$$

Here, Scale-Inv- χ^2 stand for the scaled inverse chi-square distribution. In Eq. (3), $(\mathbf{X}'\mathbf{X})^{-1}\mathbf{X}'\mathbf{Z}$ and $(\mathbf{X}'\mathbf{X})^{-1}\sigma^2$ is a mean vector and a covariance matrix for multivariate normal distribution, respectively, and N and $\frac{1}{N}(\mathbf{Z}-\mathbf{X}\boldsymbol{\beta})'(\mathbf{Z}-\mathbf{X}\boldsymbol{\beta})$ is a degree of freedom and a scale parameter for the scaled inverse chi-square distribution, respectively. The parameters $(\mathbf{Z}, \boldsymbol{\beta},$ and $\sigma^2)$ are randomly sampled and updated from the above probability distributions using the Monte Carlo Markov Chain (Gibbs sampling). The posterior distributions of any hidden variable Z are conditionally independent from each other given the model parameters $\boldsymbol{\beta}$ and σ^2 . Therefore, with the newly observed predictor set $\tilde{\mathbf{X}}=[1, \tilde{X}_{i1}, \tilde{X}_{i2}, \dots, \tilde{X}_{iK}]$, the predictive distribution for the latent variable \tilde{Z} and TC counts \tilde{h} will be

$$P(\tilde{Z} | \tilde{\mathbf{X}}, \mathbf{X}, \mathbf{h}) = \iint_{\boldsymbol{\beta}, \sigma^2} P(\tilde{Z} | \tilde{\mathbf{X}}, \boldsymbol{\beta}, \sigma^2) P(\boldsymbol{\beta}, \sigma^2 | \mathbf{X}, \mathbf{h}) d\boldsymbol{\beta} d\sigma^2$$

and

$$P(\tilde{h} | \tilde{\mathbf{X}}, \mathbf{X}, \mathbf{h}) = \int_{\tilde{Z}} \frac{\exp(-e^{\tilde{Z}} + \tilde{Z}\tilde{h})}{\tilde{h}!} P(\tilde{Z} | \tilde{\mathbf{X}}, \mathbf{X}, \mathbf{h}) d\tilde{Z}. \quad (4)$$

Even with the non-informative prior, the posterior distribution of the model parameter set $(\boldsymbol{\beta}, \sigma^2)$ in Eq. (4) is still not the standard distribution and directly sampling from it is difficult. In this section, we design a Gibbs sampler that has a stationary distribution of $P(\boldsymbol{\beta}, \sigma^2 | \mathbf{X}, \mathbf{h})$; we then use an alternative approach to integrate Eq. (4):

$$P(\tilde{Z} | \tilde{\mathbf{X}}, \mathbf{X}, \mathbf{h}) = \frac{1}{L} \sum_{i=1}^L P(\tilde{Z} | \tilde{\mathbf{X}}, (\boldsymbol{\beta}, \sigma^2)^{[i]}), \quad (5a)$$

$$P(\tilde{h} | \tilde{\mathbf{X}}, \mathbf{X}, \mathbf{h}) = \frac{1}{L} \sum_{i=1}^L \frac{\exp(-e^{\tilde{Z}^{[i]}} + \tilde{Z}^{[i]}\tilde{h})}{\tilde{h}!}, \quad (5b)$$

where $(\boldsymbol{\beta}, \sigma^2)^{[i]}$ is the i -th sampling from the proposed Gibbs sampler after the burn-in period, $\tilde{Z}^{[i]}$ is subsequently sampled from $\tilde{Z}^{[i]} | \tilde{\mathbf{X}}, (\boldsymbol{\beta}, \sigma^2)^{[i]} \sim \text{Normal}$

$(\tilde{Z}^{[i]} | \tilde{\mathbf{X}}\boldsymbol{\beta}^{[i]}, \sigma^{2[i]})$ and L is sufficiently large. In this study, the first 2000 iterations are considered the burn-in period and the following 8000 samples are used as the output of the Gibbs sampler.

4. Seasonal predictions and validations

A common way to verify the prediction method is to apply a cross-validation test for the dataset in hand. Because the seasonal TC variation is nearly independent from year to year, it is proper to apply the leave-one-out cross validation (e.g., Gray *et al.* 1992; Chu *et al.*, 2007). Specifically, a target year is chosen and a model is developed using the remaining portion of the data as the training set. The observations of the selected predictors for the target year are then served as inputs to forecast the missing year. This process is repeated successively until all N (i.e., sample size) years are forecast. In the context of Bayesian regression approach as outlined in section 3c, cross-validation is taken by the following steps. For forecasting a target year, say the j -th year, we use the other $N-1$ years' observations except for the target year as the training data for the input of Gibbs sampler which is proposed in Eq. (3). As a result, we obtain the model parameters $\boldsymbol{\beta}^{[i]}$ and $\sigma^{2[i]}$ for i -th iteration after the burn-in period from the Gibbs sampler using the training data set. With the predictor set for the forecasting year, i.e., $\tilde{\mathbf{X}}_j = [1, \tilde{X}_{j1}, \tilde{X}_{j2}, \tilde{X}_{j3}] = [1, \text{SST}_j, \text{VOR850}_j, \text{OLR}_j]$ we then sample the predictive variable $\tilde{Z}_j^{[i]}$ for a forecasting year from a normal distribution with the mean $\tilde{\mathbf{X}}_j\boldsymbol{\beta}^{[i]}$ (that is, $\beta_0^{[i]} + \text{SST}_j\beta_1^{[i]} + \text{VOR850}_j\beta_2^{[i]} + \text{OLR}_j\beta_3^{[i]}$) and the variance $\sigma^{2[i]}$. This provides the posterior sample of $\tilde{\lambda}^{[i]} = \exp(\tilde{Z}_j^{[i]})$. Subsequently, we use Eq. (5b) to compute the posterior predictive distribution of the TC counts (\tilde{h}) for the target year. We perform the cross-validation only for 1979–2003. The TC prediction for the independent period (2004–2007) is also similar to the method before 2003. One difference is that the past data up to one year prior to a forecasting year are used as the training data set for the Gibbs sampler for those four years, e.g., use of the data up to 2005 for the 2006 prediction.

Figure 4 shows the time series of TCs over the ECS

taken from observation and the mean, upper quartile, and lower quartile of the 8000 samples of predicted TC counts (\tilde{h}) for each year using the Bayesian prediction system. Figures 4a and 4b are for the extended and peak season forecasts, respectively. Here, the mean of the predicted samples indicates the expected number of TCs for each year. The distance between the upper and lower quartiles indicates the central 50% of the prediction range. In Figs. 4a and 4b, cross-validation results for the period 1979–2003 and the prediction results for the independent period 2004–2007 are shown.

Generally, the difference between the observed and predicted TCs fluctuates in phase with strong interannual variations. Only 4 years fall outside the central 50% of the prediction range for the extended season forecast (Fig. 4a), and only 5 years fall outside that range for the peak season forecast over the entire 29 years (Fig. 4b). For the entire period, the correlation coefficients between the observations and the

mean predictions are 0.69 for the extended season forecast and 0.71 for the peak season forecast, which are both significant at the 99.9% confidence level. However, a large discrepancy is found for 2004 when a record high number of TCs occurred in the ECS; 4.5 TCs were predicted for the extended season and 5.3 for the peak season, whereas the observed were 10 and 8 TCs, respectively. This indicates that our predictors did not capture important physics for TC variations during this exceptional year.

The accuracy of the deterministic prediction method using the mean of predictions is assessed based on the root mean square error (RMSE) and the mean square skill score (MSSS). During the entire period, the RMSE is 1.48 for the extended season prediction and 1.20 for the peak season prediction. The RSME is relatively small for the cross-validation period (1.17 for the extended season and 1.15 for the peak season), but it tends to be larger during the independent period (2.79 for the extended season and

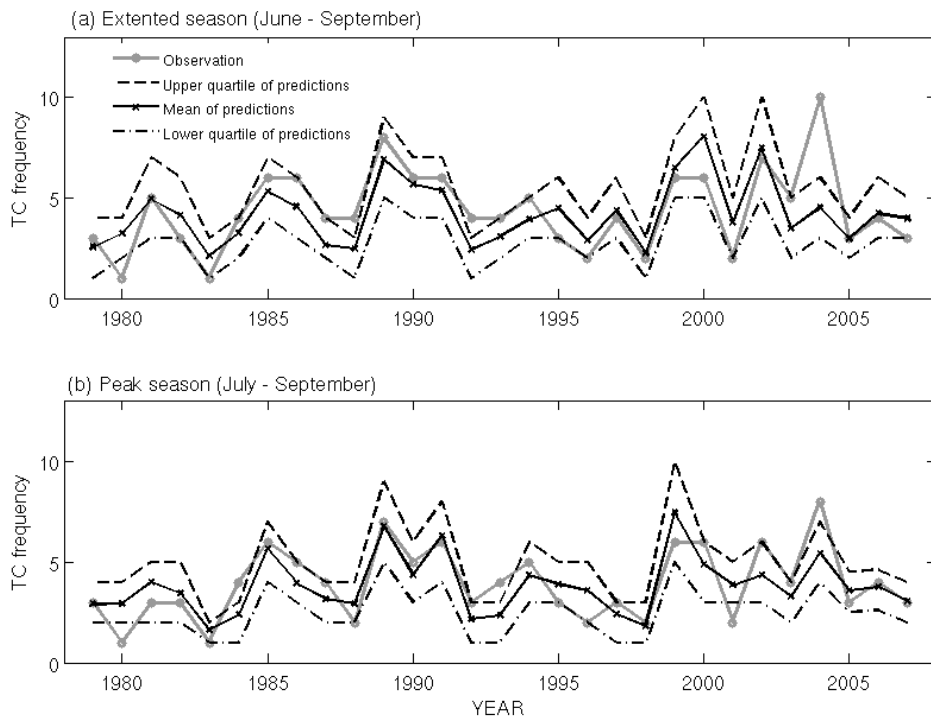


Fig. 4. Time series of the mean (dark solid line), and upper and lower quartiles (broken lines) of the cross-validated prediction of TC counts over the Eastern China Sea for (a) the extended season and (b) the peak season. The actual observed TC counts are shown as opaque solid lines.

1.48 for the peak season forecast, respectively) because of the large error in 2004. The MSSS is defined as the ratio of the reduction in the mean square error of the predictions to the reference forecasts based on the climatology value (WMO, 2002). The MSSS is 0.50 for the extended season forecasts and 0.57 for the peak season forecasts. Based on the MSSS, this method is 50% more accurate than the reference forecast. Moreover, the results show that the predictions for the peak season are slightly more skillful than the predictions for the extended season. It is noted that the deterministic prediction results using the mean value of the Bayesian prediction are nearly same with the results using the ordinary Poisson regression because the present Bayesian model is based on the Poisson regression. The advantage of the Bayesian approach is the probabilistic prediction with probable forecasting ranges as shown in Fig. 4, while the Poisson regression provides the deterministic prediction values.

Other than the present prediction method, the smart predictors were used for skillful predictions of seasonal TC activity over the WNP (e.g., Lee *et al.*, 2007; Kwon *et al.*, 2007). The smart predictors refer to a combination of several predictors among numerous potential predictors, yielding the best prediction performance during the hindcast period. However, the smart predictors are not adopted in this study because we use only three predictors averaged over significantly correlated regions. While the smart predictor is not employed in this study, the Bayesian prediction results seem to provide skillful performance to forecast the TC frequency over the ECS.

5. Summary

This study used the Bayesian method to predict the seasonal number of TCs over the ECS. TC predictions were made for two periods each year: one, made on June 1, was an extended season forecast that covered the time period of June–September, and the other, made on July 1, was a peak season forecast that covered the time period of July–September. Three climate parameters, SST, OLR, and VOR850, were used as predictors in both cases; they were determined through lagged-correlation analysis. For

the extended season forecast issued June 1, the remote SST in the three significantly correlated regions over the Pacific for February–April was adopted. The VOR850 data that were averaged over the critical region in the western Pacific for April 16–May 15 were also used. Likewise, the significantly correlated OLR data recorded in the tropical western North Pacific region between March 16 and May 15 were used. Overall, data consisting of the three parameters collected in a similar geographical range were chosen as the predictors to be used for the peak season forecast. The data used in the peak season forecast were one month new compared to the extended season forecast.

The predicted TCs for both the extended and peak seasons vary in a manner similar to that of the observed TCs. Using the mean values of the predicted TCs, the cross-validated correlation coefficients between the predicted and observed TCs are 0.69 for the extended season forecast and 0.71 for the peak season forecast. These are both significant at the 99.9% confidence level. Given the correlation coefficients and MSSS, the Bayesian method yields an improvement of more than 50% over the reference forecast method. In particular, the Bayesian method has the advantage that it offers several different predictions on the number of TCs that will occur in the typhoon season, each with a probability assigned to it. This is superior to previous methods that predicted only a deterministic value. The present forecast system is being considered by the Korean Meteorological Administration as an operational tool.

Acknowledgement. This work was funded by the Korea Meteorological Administration Research and Development Program under Grant CATER 2006–4204. Hyeong-Seog Kim was supported by the BK21 Project of the Korean government. The authors sincerely thank two anonymous reviewers for the critical valuable comments.

REFERENCES

- Chan, J. C. L., J.-E. Shi, and C.-M. Lam, 1998: Seasonal forecasting of tropical cyclone activity over the western North Pacific and the South China Sea. *Wea.*

- Forecasting*, **13**, 997–1004.
- _____, _____, and K. S. Liu, 2001: Improvements in the seasonal forecasting of tropical cyclone activity over the western North Pacific. *Wea. Forecasting*, **16**, 491–498.
- Chu, P.-S. and J. X. Wang, 1998: Modeling return periods of tropical cyclone intensities in the vicinity of Hawaii. *J. Appl. Meteor.*, **37**, 951–960.
- _____, 2004: ENSO and tropical cyclone activity. In *Hurricane and Typhoon: Past, Present, and Future*, Eds. R. J. Murnane and K. B. Liu, Columbia Univ. Press: New York, 462 pp.
- _____, X. Zhao, C.-T. Lee, and M.-M. Lu, 2007: Climate prediction of tropical cyclone activity in the vicinity of Taiwan using the multivariate least absolute deviation regression method. *Terr. Atmos. Oceanic Sci.*, **18**, 805–825.
- _____, and _____, 2007: A Bayesian regression approach for predicting seasonal tropical cyclone activity over the central North Pacific. *J. Climate*, **20**, 4002–4012.
- Elsner, J. B., and T. H. Jagger, 2006: Prediction models for annual U.S. hurricane counts. *J. Climate*, **19**, 2935–2952.
- Epstein, E.-S., 1985: *Statistical Inference and Prediction in Climatology: A Bayesian Approach*. Meteor. Monogr., No. 42, Amer. Meteor. Soc., 199 pp.
- Gray, W. M., C. W. Landsea, P. W. Mielke, and K. J. Berry, 1992: Predicting Atlantic seasonal hurricane activity 6–11 months in advance. *Wea. Forecasting*, **7**, 440–455.
- Harrison, D. E. and N. K. Larkin, 1998: El Niño–Southern Oscillation sea surface temperature and wind anomalies 1946–1993. *Rev. Geophys.*, **36**, 353–399.
- Ho, C.-H., J.-J. Baik, J.-H. Kim, D.-Y. Gong, and C.-H. Sui, 2004: Interdecadal changes in summertime typhoon tracks. *J. Climate*, **17**, 1767–1776.
- _____, J.-H. Kim, H.-S. Kim, C.-H. Sui, and D.-Y. Gong, 2005: Possible influence of the Antarctic Oscillation on tropical cyclone activity in the western North Pacific. *J. Geophys. Res.*, **110**, D19104.
- Kanamitsu, M., W. Ebisuzaki, J. Woollen, S.-K. Yang, J. Hnilo, M. Fiorino, and G. L. Potter, 2002: NCEP–DOE AMIP-2 Reanalysis (R-2). *Bull. Amer. Meteor. Soc.*, **83**, 1631–1643.
- Kim, J.-H., C.-H. Ho, and C.-H. Sui, 2005a: Circulation features associated with the record-breaking typhoon landfall on Japan in 2004. *Geophys. Res. Lett.*, **32**, L14713.
- _____, _____, C.-H. Sui, and S.-K. Park, 2005b: Dipole structure of interannual variations in summertime tropical cyclone activity over East Asia. *J. Climate*, **18**, 5344–5356.
- Kwon H. J., W.-J. Lee, S.-H. Won, and E.-J. Cha, 2007: Statistical ensemble prediction of the tropical cyclone activity over the western North Pacific. *Geophys. Res. Lett.*, **34**, L24805.
- Lee, W.-J., J.-S. Park, and H. J. Kwon, 2007: A statistical model for prediction of the tropical cyclone activity over the western North Pacific. *J. Korean Meteor. Soc.*, **43**, 175–183.
- Liebmann, B., and C. A. Smith, 1996: Description of a complete (interpolated) outgoing longwave radiation dataset. *Bull. Amer. Meteor. Soc.*, **77**, 1275–1277.
- Liu, K. S., and J. C. L. Chan, 2003: Climatological characteristics and seasonal forecasting of tropical cyclones making landfall along the South China coast. *Mon. Wea. Rev.*, **131**, 1650–1662.
- Nakazawa T., 2006: Madden-Julian oscillation activity and typhoon landfall on Japan in 2004. *Sci. Online Lett. Atmos.*, **2**, 136–139, doi: 10.2151/sola.2006-035.
- NEMA, 2008: 2008 Essential Statistics and Data. National Emergency Management Agency, 383 pp. [Available online at <http://www.nema.go.kr/data/statistic/list.jsp>] (In Korean).
- Smith, T. M., R.W. Reynolds, T. C. Peterson, and J. Lawrimore, 2007: Improvements to NOAA's historical merged land-ocean surface temperature analysis (1880–2006). *J. Climate*, **21**, 2283–2296.
- Wang, B., R. Wu, and K.-M. Lau, 2001: Interannual variability of Asian summer monsoon: Contrast between the Indian and western North Pacific–East Asian monsoons. *J. Climate*, **14**, 4073–4090.
- Wang, B., Y. Xu, and B. Bi, 2007: Forecasting and warning of tropical cyclone in China. *Data Sci. J.*, **6**, S723–S737. doi:10.2481/dsj.6.S723.
- WMO, 2002: Standardized verification system for long-range forecasts, New attachment II-9 to the manual on the GDPFS. WMO No. 485, World Meteorological Organization, 22 pp.